Journal of Sound and Vibration (1997) **204**(2), 311–329

NATURAL FREQUENCIES OF HELICAL SPRINGS OF ARBITRARY SHAPE

V. YILDIRIM AND N. İNCE

Department of Mechanical Engineering, Çukorova University, 01330 *Balcalı, Adana, Turkey*

(*Received* 6 *August* 1996, *and in final form* 31 *January* 1997)

The natural frequencies of helical springs having arbitrary shapes, such as conical, barrel and hyperboloidal, are obtained by the transfer matrix method using the distributed mass model and Timoshenko's beam theory together with the axial deformation. The governing equations of cylindrical helical springs are applied to free vibration analysis of non-cylindrical helices. It is shown that the present numerical results agree well with the previously published ones which have been obtained both theoretically and experimentally. A comparison of natural frequencies of non-cylindrical helices is made. For the circular section, the effects of the helix pitch angle, the number of active turns, the ratio of diameters of the minimum cylinder to the maximum cylinder, and the ratio of diameters of maximum cylinder to the diameter of wire on the free vibration frequencies of all types of helices are investigated. The effects of axial and shear deformations, and the rotary inertia are also studied.

1. INTRODUCTION

Helical springs having cylindrical or non-cylindrical shapes are fundamental elements of machines. Although the undamped free vibration problems of cylindrical coil springs have been reported by many researchers [1–21], there have been only a few studies on the free vibration of helical springs of irregular shapes [22–25]. Epstein [22] has theoretically obtained the fundamental frequency for conical coil springs for several boundary conditions. Nagaya *et al*. [23] have determined the free vibration frequencies of non-cylindrical helical springs both experimentally and by the method of Myklestad. For this purpose, they have used the static element transfer matrix, which they derived in closed form taking into account only the axial deformation for circular cross-sections. The Myklestad method has also been employed in Yıldırım's study [24], including the rotary inertia, the axial and the shear deformation terms in the free vibrational analysis of irregular helices. Using both the transfer matrix and the complementary functions methods, Yıldırım [25] has studied the free vibration of non-cylindrical helical springs. Yıldırım [25] has presented the first ten exact natural frequencies for circular and squared sections in graphical forms.

In this study, the problem of free vibration of non-cylindrical coil springs is numerically treated with the help of the transfer matrix method. An efficient numerical algorithm is employed for the computation of the element transfer matrix. The helix is considered as a continuous system and the Timoshenko beam theory is employed. The first three natural

0022–460X/97/270311 + 19 $25.00/0/sv970940

frequencies are computed and the results are presented for all the helix types used in practice.

2. FREE VIBRATION EQUATIONS OF NON-CYLINDRICAL HELICAL SPRINGS

Frenet unit vectors are defined as follows:

$$\mathbf{t} = \frac{\mathrm{d}\mathbf{r}}{\mathrm{d}s}, \qquad \mathbf{n} = \frac{\mathrm{d}\mathbf{t}/\mathrm{d}s}{\mathrm{d}t/\mathrm{d}s}, \qquad \mathbf{b} = \mathbf{t} \times \mathbf{n}, \tag{1}$$

where ds is the infinitesimal arc length along the curve and $\mathbf{r}$ is the position vector. $\mathbf{t}$ is the tangential, $\mathbf{n}$ is the normal and $\mathbf{b}$ is the binormal unit vector. The relations among these unit vectors are

$$\frac{\mathrm{d}\mathbf{t}}{\mathrm{d}s} = \chi\mathbf{n}, \qquad \frac{\mathrm{d}\mathbf{n}}{\mathrm{d}s} = \tau\mathbf{b} - \chi\mathbf{t}, \qquad \frac{\mathrm{d}\mathbf{b}}{\mathrm{d}s} = -\tau\mathbf{n}. \tag{2}$$

Here, χ and τ are the curvature and the torsion of the wire axis, respectively.

The governing equations of spatial bars in canonical form in Frenet co-ordinates have been given by Yıldırım [21] as

$$\partial U_t/\partial s = \chi U_n + (1/EA)T_t, \qquad \partial U_n/\partial s = -\chi U_t + \tau U_b + \Omega_b + (\alpha_n/GA)T_n, \tag{3a, b}$$

$$\partial U_b/\partial s = -\tau U_n - \Omega_n + (\alpha_b/GA)T_b, \qquad \partial \Omega_t/\partial s = \chi\Omega_n + (1/GI_t)M_t, \tag{3c, d}$$

$$\partial \Omega_n/\partial s = -\chi\Omega_t + \tau\Omega_b + (1/EI_n)M_n, \qquad \partial \Omega_b/\partial s = -\tau\Omega_n + (1/EI_b)M_b, \tag{3e, f}$$

$$\partial T_t/\partial s = \chi T_n - p_t + (\rho A)(\partial^2 U_t/\partial t^2), \qquad \partial T_n/\partial s = -\chi T_t + \tau T_b - p_n + (\rho A)(\partial^2 U_n/\partial t^2), \tag{3g, h}$$

$$\partial T_b/\partial s = -\tau T_n - p_b + (\rho A)(\partial^2 U_b/\partial t^2), \qquad \partial M_t/\partial s = \chi M_n - m_t + (\rho I_t)(\partial^2 \Omega_t/\partial t^2), \tag{3i, j}$$

$$\partial M_n/\partial s = T_b - \chi M_t + \tau M_b - m_n + (\rho I_n)(\partial^2 \Omega_t/\partial t^2),$$

$$\partial M_b/\partial s = -T_n - \tau M_n - m_b + (\rho I_b)(\partial^2 \Omega_b/\partial t^2), \tag{3k, l}$$

where T_t, T_n and T_b are the components of the internal forces on the cross-section in the $\mathbf{t}$, $\mathbf{n}$, and $\mathbf{b}$ directions, and M_t, M_n and M_b are the components of the internal moments on this section in the $\mathbf{t}$, $\mathbf{n}$, and $\mathbf{b}$ directions, respectively. Similarly, U_t, U_n, U_b and $\Omega_t, \Omega_n, \Omega_b$ are the Frenet components of the displacement and rotational vectors, respectively. E and G are the Young's modulus and shear modulus of the material, respectively. A is the cross-sectional area, I_n and I_b are the moments of inertia about the $\mathbf{n}$ and $\mathbf{b}$ axes, respectively. α_n and α_b are Timoshenko's coefficients, I_t is the torsional moment of inertia, ρ is the density of the material, and t is the time.

The assumptions that the centroid of the cross-section and the shear center are coincident, the ($\mathbf{n}$, $\mathbf{b}$) axes are the principal axes of the cross-section, warping is neglected and, furthermore, the bar has an elastic, homogeneous and isotropic material are used in equations (3).

Defining the state vector as,

$$\{S(s, t)\} = \{U_t, U_n, U_b, \Omega_t, \Omega_n, \Omega_b, \ T_t, T_n, T_b, \ M_t, M_n, M_b\}^{\mathrm{T}}, \tag{4}$$

equations (3) can be written in a compact form,

$$\frac{\partial\{S(s,t)\}}{\partial s} = [A]\{S(s,t)\} + [B]\frac{\partial^2\{S(s,t)\}}{\partial t^2} + \{P(s,t)\}, \tag{5}$$

where $[A]$ is referred to as the differential matrix and $\{P\}$ is the load vector. In equation (5), $[A]$, $\{P\}$ and $\{S\}$ are functions of both s and t.

Denoting the angular frequency by ω, a harmonic solution in the form of

$$\{S(s,t)\} = \{S^0(s)\}\sin(\omega t) \tag{6}$$

can be assumed for free vibrations. Substituting this solution into equation (5) and setting the external loads equal to zero, $\{P\} = \{0\}$, the following equation can be obtained:

$$\frac{\mathrm{d}\{S^0(s)\}}{\mathrm{d}s} = [A^0(\omega, s)]\{S^0(\mathrm{s})\}, \tag{7}$$

where the superscript zero denotes that the quantity is only a function of the co-ordinate s.

Determining the exact differential equations of non-cylindrical helical springs and their solution is laborious. In the present study, this problem is handled with the help of the equations of cylindrical helices. Since the curvatures of non-cylindrical helices vary along the axis, the bar has been formed by the cylindrical helical elements attached sequentially to each other. Constant but different curvature is assumed for each element. Hence, the effective approximate solution for non-cylindrical helices can be obtained using fewer elements. It is clear that if the number of elements is increased, the approximate solution will converge rapidly to the exact solution.

The geometrical properties of a cylindrical helix are (see Figure 1)

$$h = R\tan\alpha, \qquad c = (R^2 + h^2)^{1/2}, \qquad \tau = h/c^2 = (1/R)\sin\alpha\cos\alpha,$$
$$\chi = R/c^2 = (1/R)\cos^2\alpha, \qquad \mathrm{d}s = c\,\mathrm{d}\theta, \tag{8a–e}$$

where h is the step for unit angle of the helix, R is the centreline radius of the helix, α is the pitch angle and $\mathrm{d}\theta$ is the infinitesimal angular element.

The horizontal radius of any point that lies on the axis of the bar is determined for barrel and hyperboloidal types of helices from

$$R = R_1 + (R_2 - R_1)\left(1 - \frac{\theta}{\pi n_c}\right)^2, \tag{9}$$

and for conical springs (see Figure 2) from

$$R = R_1 + \frac{(R_2 - R_1)\theta}{2\pi n_c}, \tag{10}$$

where n_c is the number of active turns.

Although the pitch angle of helices is considered constant, the values c, h and R will be varied along the axis for the non-cylindrical helix. Thus, the fixed reference value, R_0, which can be selected arbitrarily, has been used for obtaining the differential equations in non-dimensional form

$$c_0^2 = R_0^2 + h_0^2, \qquad h_0 = R_0\tan\alpha. \tag{11}$$

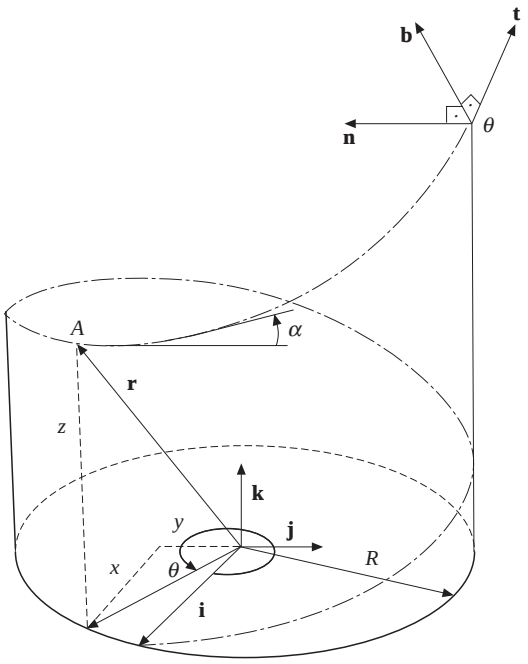

Figure 1. The geometrical properties of a cylindrical helix and Frenet co-ordinates.

The dimensionless groups for the elements of the state vector at any section of the bar are determined as follows:

$$\bar{T}_i^0 = \frac{c_0^2}{EI_n} T_i^0, \qquad \bar{M}_i^0 = \frac{c_0}{EI_n} M_i^0, \qquad \bar{U}_i^0 = \frac{1}{c_0} U_i^0, \qquad \bar{\Omega}_i^0 = \Omega_i^0, \qquad (i = t, n, b). \quad (12)$$

Using equations (8), (11) and (12), a set of non-dimensional scalar equations for the non-cylindrical helix having any double symmetrical cross-sections can be written, as

$$\frac{\mathrm{d}\bar{U}_t^0}{\mathrm{d}\theta} = \frac{R}{c}\bar{U}_n^0 + \frac{I_n c}{Ac_0^3}\bar{T}_t^0, \qquad \frac{\mathrm{d}\bar{U}_n^0}{\mathrm{d}\theta} = -\frac{R}{c}\bar{U}_t^0 + \frac{h}{c}\bar{U}_b^0 + \frac{c}{c_0}\bar{\Omega}_b^0 + \frac{\alpha_n EI_n c}{GAc_0^3}\bar{T}_n^0, \quad (13a, b)$$

$$\frac{\mathrm{d}\bar{U}_b^0}{\mathrm{d}\theta} = -\frac{h}{c}\bar{U}_n^0 - \frac{c}{c_0}\bar{\Omega}_n^0 + \frac{\alpha_b EI_n c}{GAc_0^3}\bar{T}_b^0, \qquad \frac{\mathrm{d}\bar{\Omega}_t^0}{\mathrm{d}\theta} = \frac{R}{c}\bar{\Omega}_n^0 + \frac{EI_n c}{GI_t c_0}\bar{M}_t^0, \quad (13c, d)$$

$$\frac{\mathrm{d}\bar{\Omega}_n^0}{\mathrm{d}\theta} = -\frac{R}{c}\bar{\Omega}_t^0 + \frac{h}{c}\bar{\Omega}_b^0 + \frac{c}{c_0}\bar{M}_n^0, \qquad \frac{\mathrm{d}\bar{\Omega}_b^0}{\mathrm{d}\theta} = -\frac{h}{c}\bar{\Omega}_n^0 + \frac{I_n c}{I_b c_0}\bar{M}_b^0, \quad (13e, f)$$

$$\frac{\mathrm{d}\bar{T}_t^0}{\mathrm{d}\theta} = -\frac{\rho Ac_0^3 c\omega^2}{EI_n}\bar{U}_t^0 + \frac{R}{c}\bar{T}_n^0, \qquad \frac{\mathrm{d}\bar{T}_n^0}{\mathrm{d}\theta} = -\frac{\rho Ac_0^3 c\omega^2}{EI_n}\bar{U}_n^0 - \frac{R}{c}\bar{T}_t^0 + \frac{h}{c}\bar{T}_b^0, \quad (13g, h)$$

$$\frac{\mathrm{d}\bar{T}_b^0}{\mathrm{d}\theta} = -\frac{\rho Ac_0^3 c\omega^2}{EI_n}\bar{U}_b^0 - \frac{h}{c}\bar{T}_n^0, \qquad \frac{\mathrm{d}\bar{M}_t^0}{\mathrm{d}\theta} = -\frac{\rho\omega^2 I_t c_0 c}{EI_n}\bar{\Omega}_t^0 + \frac{R}{c}\bar{M}_n^0, \quad (13i, j)$$

$$\frac{\mathrm{d}\bar{M}_n^0}{\mathrm{d}\theta} = -\frac{\rho\omega^2 c_0 c}{E}\bar{\Omega}_n^0 + \frac{c}{c_0}\bar{T}_b^0 - \frac{R}{c}\bar{M}_t^0 + \frac{h}{c}\bar{M}_b^0, \qquad \frac{\mathrm{d}\bar{M}_b^0}{\mathrm{d}\theta} = -\frac{\rho\omega^2 I_b c_0 c}{EI_n}\bar{\Omega}_b^0 - \frac{c}{c_0}\bar{T}_n^0 - \frac{h}{c}\bar{M}_n^0. \quad (13k, l)$$

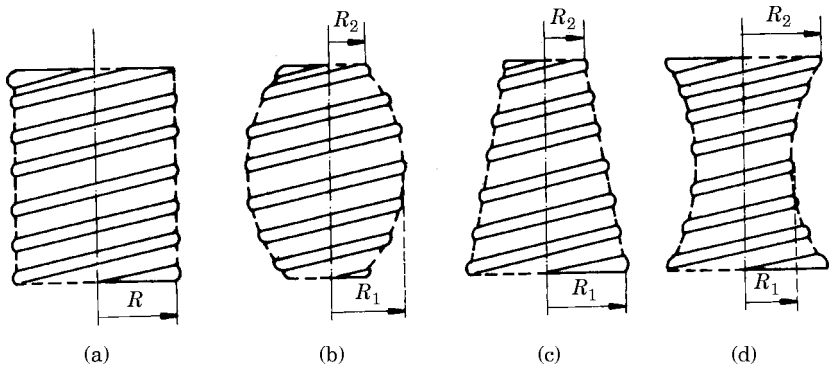

Figure 2. The different shapes of helical springs. (a) Cylindrical; (b) barrel; (c) conical; (d) hyperboloidal.

For the cylindrical springs, it was proved that the coefficients of the odd powers of the differential matrix, which is available from equations (13), in the characteristics determinant of $[A^0]$ are equal to zero [20, 21]:

$$[A^0]^{12} - p_1[A^0]^{10} - p_2[A^0]^8 - \cdots - p_5[A^0]^2 - p_6[I] = [0], \tag{14}$$

where $[I]$ is the unit matrix and $[A^0]^i$ is the powers of the differential matrix.

Homogeneous solution of equation (13) associated with the dynamic transfer matrix, $[F]$, is given as follows:

$$\{S^0(\theta)\} = [F(\theta, \omega)]\{S^0(0)\}. \tag{15}$$

Since the curvatures, the material and the cross-section are not changed along the axis, the elements of the differential matrix will be constant (not a function of length) for cylindrical helical bars. In this case, the transfer matrix can be numerically obtained from the standard solution, which is in the form of series:

$$[F] = e^{\theta[A^0]} = [I] + \theta[A^0] + \frac{\theta^2[A^0]^2}{2!} + \frac{\theta^3[A^0]^3}{3!} + \cdots \tag{16}$$

The infinite and convergent [26] series can be used for determination of the element transfer matrix as it is, if the pitch angle is small and the system is less rigid. To obtain

TABLE 1

Dimensionless frequencies, μ, of the cylindrical helical spring of both edges built in ($d = 8\ mm$, $R = 26\ mm$, $n_c = 6{\cdot}5$, $\alpha = 4{\cdot}8^\circ$, $\rho = 7850\ kg/m^3$, $E = 2{\cdot}1 \times 10^{11}\ N/m^2$, $v = 0{\cdot}3$, $\alpha_n = \alpha_b = 1{\cdot}1$)

$\mu = R(\rho/G)^{1/2}$	μ_1	μ_2	μ_3	μ_4
Nagaya *et al*. [23] (78 elements), including rotary inertia, including axial deformation	0·00835	0·00914	0·01039	0·01063
Nagaya *et al*. [23] (78 elements), excluding rotary inertia, including axial deformation	0·00835	0·00925	0·01039	0·01065
Sawanobori and Fukishima [23], finite element method	0·00826	0·00923	0·01038	0·01056
Present study (five elements)	0·008254	0·009208	0·010342	0·010536

TABLE 2

Variation of the theoretical frequencies (in Hertz) with the number of elements for the hyperboloidal type spring having the ratio of $R_2/R_1 = 2{\cdot}4$

	Number of elements												
Modes	15	20	25	30	35	40	45	50	60	70	80	100	200
1	76·06	75·97	75·91	75·86	75·84	75·82	75·81	75·80	75·79	75·78	75.78	75·77	75·76
2	94·66	95·34	95·68	95·87	95·98	96·06	96·11	96·15	96·20	96·23	96·25	96·27	96·30
3	102·54	102·91	103·01	103·04	103·06	103·06	103·07	103·07	103·08	103·08	103·08	103·08	103·09
4	129·69	131·11	131·83	132·24	132·49	132·66	132·77	132·85	132·96	133·03	133·07	133·12	133·13

the overall transfer matrix, the rod is divided into small elements having equal lengths (or angles) and in this case equation (17) is used:

$$[F]_{system} = [F]^m_{element}, \tag{17}$$

where m is the number of small elements. In the case of cylindrical helices, the element transfer matrices are identical and need be computed only once. The overall transfer matrix can then be calculated with sequential matrix multiplications as in equation (17).

Although the horizontal angles of the elements of non-cylindrical helices are chosen to be equal, the element transfer matrices will not be identical owing to varying radii. In this case, the transfer matrix of each element must be computed. As a result, the required time for computation of the overall transfer matrix increases depending on the number of elements.

TABLE 3

Natural frequencies (in Hertz) of hyperboloidal spring for various ratios of R_2/R_1

	Modes						
	1	2	3	4	5	6	R_2/R_1
	211·5	235·5	265·1	269·9	413·3	438·5	1·0
Yıldırım [24]	178·8	208·7	227·7	238·3	359·9	376·5	1·2
(50 elements)	130·1	159·3	170·5	193·2	270·6	287·2	1·6
	97·7	122·2	130·8	159·3	205·5	227·4	2·0
	75·6	95·8	102·8	132·2	160·7	181·7	2·4
	210·0	233·0	262·0	270·0	—	—	1·0
Nagaya *et al*. [23]	178·0	205·0	225·0	238·0	—	—	1·2
(78 elements),	130·0	157·0	171·0	193·0	—	—	1·6
(theoretical)	99·0	121·0	131·0	159·0	—	—	2·0
	76·0	96·0	103·0	133·0	—	—	2·4
	212·0	236·0	264·0	274·0	—	—	1·0
Nagaya *et al*. [23],	178·0	216·0	232·0	240·0	—	—	1·2
(experimental)	128·0	158·0	172·0	192·0	—	—	1·6
	96·0	114·0	128·0	160·0	—	—	2·0
	211·48	235·49	265·05	269·94	413·26	438·52	1·0
Present study	178·91	208·76	227·80	238·41	360·01	376·70	1·2
(50 elements)	130·27	159·51	170·70	193·46	270·95	287·54	1·6
	97·87	122·54	131·03	159·79	205·69	228·00	2·0
	75·80	96·15	103·07	132·85	160·69	182·96	2·4

TABLE 4

Free vibration frequencies (in Hertz) of barrel spring of both edges built in for various ratios of R_2/R_1 ($R_1 = 25\ mm$)

	Modes						
	1	2	3	4	5	6	R_2/R_1
	71·86	81·19	99·95	99·96	143·88	—	0·2
Yıldırım [25],	65·53	71·52	86·94	87·01	129·60	—	0·4
exact	59·62	61·78	75·08	75·09	114·01	—	0·6
	52·11	54·57	64·46	64·77	99·15	—	0·8
	71·95	81·3	100·07	100·09	144·1	145·2	0·2
Yıldırım [24]	65·6	71·6	87·03	87·1	129·7	135·1	0·4
(50 elements)	59·7	61·8	75·1	75·2	114·1	120·9	0·6
	52·1	54·6	64·5	64·8	99·2	106·0	0·8
	44·1	49·0	55·3	56·3	86·1	91·4	1·0
	71·0	81·0	—	—	143·0	150·0	0·2
Nagaya *et al*. [23]	64·0	71·0	—	—	129·9	134·0	0·4
(78 elements),	59·0	60·0	—	—	113·0	120·0	0·6
(theoretical)	52·0	53·0	—	—	99.0	104·0	0·8
	43·0	48·0	—	—	85·0	90·0	1·0
	66·0	72·0	—	—	129·0	136·0	0·4
Nagaya *et al*. [23],	60·0	62·0	—	—	108·0	116·0	0·6
(experimental)	52·0	55·0	—	—	100·0	108·0	0·8
	44·0	50·0	—	—	87·0	91·0	1·0
	71·88	81·22	99·98	99·99	143·93	145·13	0·2
Present study	65·55	71·74	86·96	87·03	129·64	135·03	0·4
(50 elements)	59·63	61·80	75·08	75·12	114·04	120·84	0·6
	52·12	54·57	64·46	64·77	99·16	105·96	0·8
	44·09	49·04	55·27	56·28	86·15	91·43	1·0

TABLE 5

Natural frequencies (in Hertz) of conical spring fixed at both edges for various ratios of R_2/R_1 ($R_1 = 25\ mm$)

		Modes					
	R_2/R_1	1	2	3	4	5	6
	0·2	110·64	115·19	135·91	143·77	196·92	204·30
Present	0·4	88·84	91·82	107·52	111·52	163·01	170·96
study	0·6	69·21	74·44	85·24	87·43	131·98	138·69
	0·8	54·64	60·33	68·21	69·57	106·22	112·44
	0·2	111·8	116·4	137·4	145·4	198·9	206·4
Yıldırım	0·4	89·5	92·5	108·4	112·4	164·3	172·3
[24]	0·6	69·5	74·8	85·7	87·9	132·6	139·4
	0·8	54·8	0·5	68·4	69·7	106·5	112·7

TABLE 6

Natural frequencies (in Hertz) of hyperboloidal spring fixed at both edges for various ratios of R_1/R_2 ($R_2 = 25$ mm)

		Modes					
	R_1/R_2	1	2	3	4	5	6
	0·2	121·88	158·95	172·38	253·18	273·33	305·10
Present	0·4	92·84	118·05	126·64	165·09	197·26	225·36
study	0·6	71·66	88·16	94·30	108·29	149·39	159·76
	0·8	55·89	65·76	71·46	75·43	113·22	118·17
	0·2	121·3	157·5	171·6	248·5	276·6	299·4
Yıldırım	0·4	92·6	117·5	126·3	164·2	197·3	223·6
[24]	0·6	71·6	88·0	94·2	108·1	149·2	159·5
	0·8	55·9	65·7	71·4	75·4	113·2	118·1

3. THE OVERALL TRANSFER MATRIX FOR THE CONTINUOUS SYSTEM

In the transfer matrix method, computing of the overall transfer matrix accurately for any number of active coils, n_c, is a crucial problem. After computing it for $\theta = 2\pi n_c$, the minor of the transfer matrix is determined according to the boundary conditions given at both ends. For example, if the helical spring of both edges built in is considered, the displacements and the angles of rotation disappear at both ends. With these boundary

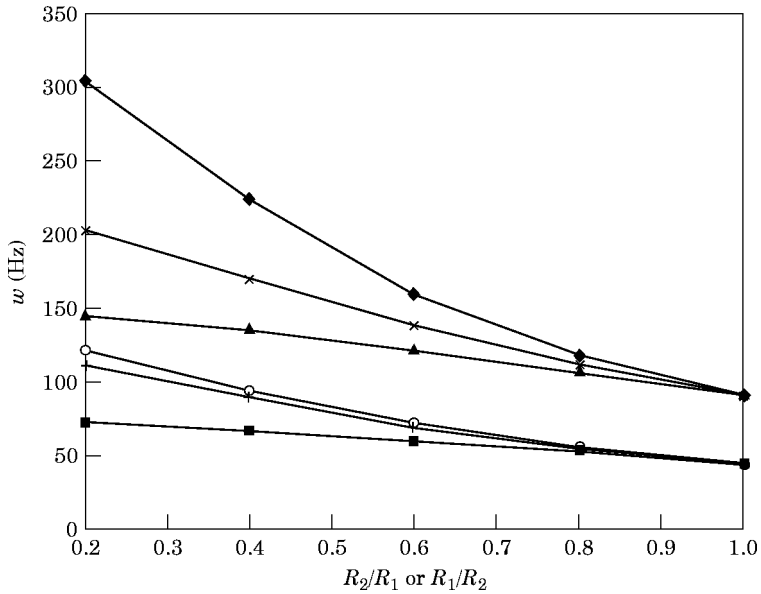

Figure 3. Variation of the frequencies associated with the first and sixth modes with respect to the types of spring. ■, Barrel (mode 1); +, conical (mode 1): ○, hyperboloidal (mode 1); ▲, barrel (mode 6); ×, conical (mode 6); ◆, hyperboloidal (mode 6).

conditions, equation (15) becomes

$$\begin{bmatrix} 0 \\ 0 \\ 0 \\ 0 \\ 0 \\ 0 \end{bmatrix}_{\theta = 2\pi n_c} = \begin{bmatrix} f_{1,7} & \cdots & f_{1,12} \\ \vdots & & \vdots \\ f_{6,7} & \cdots & f_{6,12} \end{bmatrix}_{\theta = 2\pi n_c} \begin{bmatrix} \bar{T}_t \\ \bar{T}_n \\ \bar{T}_b \\ \bar{M}_t \\ \bar{M}_n \\ \bar{M}_b \end{bmatrix}_{\theta = 0} . \tag{18}$$

The value of the circular frequency is defined by setting the determinant of the minor equal to zero. With this purpose, the different values are assigned to the angular frequency

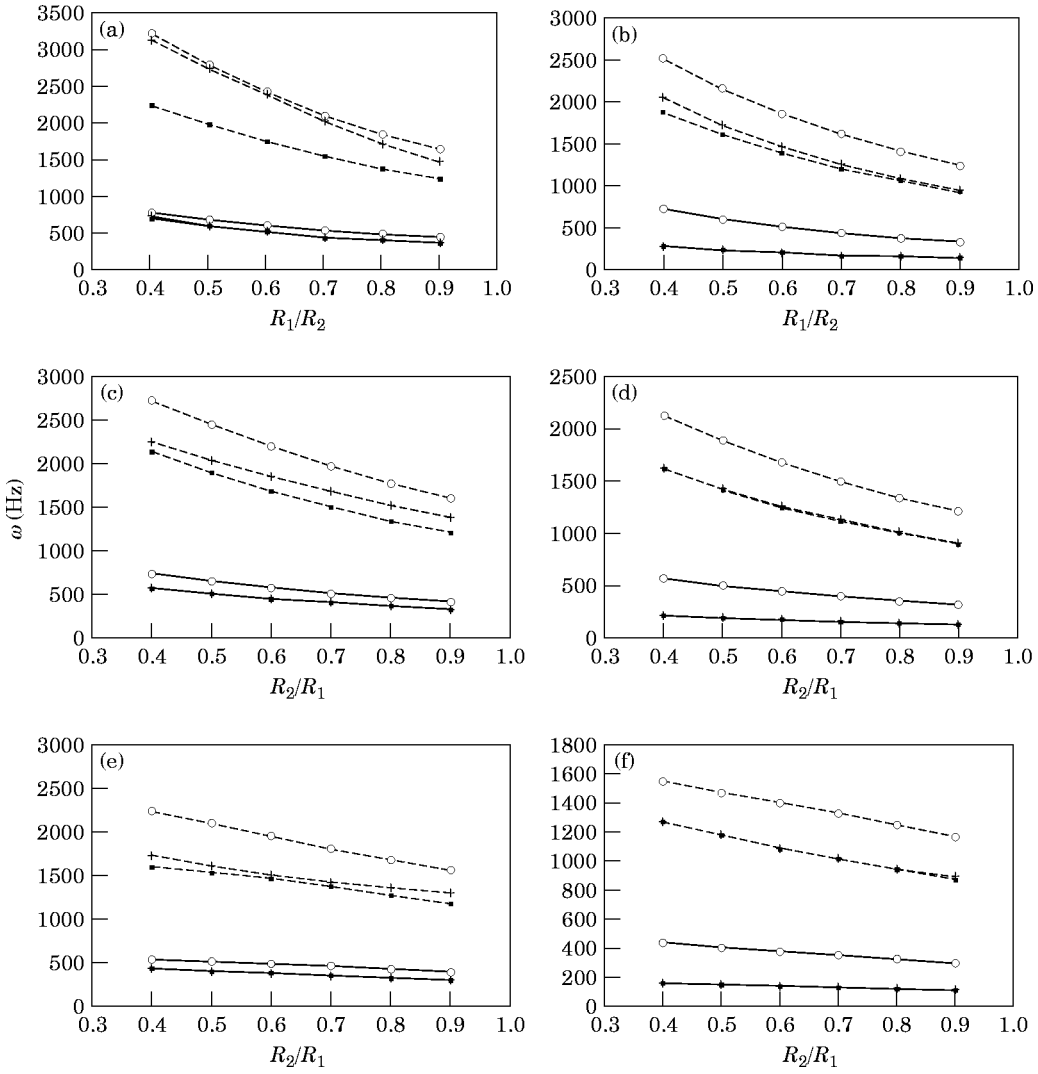

Figure 4. The effects of the helix pitch angle, the ratio R_{min}/R_{max} and the number of active turns on the natural frequencies, for $D_{max}/d = 5$. ---, $n_c = 5$; ———, $n_c = 15$. ■, ω_1; +, ω_2; ○, ω_3. (a) Hyperboloidal, $\alpha = 5°$, $D_2/d = 5$; (b) hyperboloidal, $\alpha = 15°$, $D_2/d = 5$; (c) conical, $\alpha = 5°$, $D_1/d = 5$; (d) conical, $\alpha = 15°$, $D_1/d = 5$, (e) barrel, $\alpha = 5$, $D_1/d = 5$; (f) barrel, $\alpha = 15°$, $D_1/d = 5$.

and the determinant of the minor corresponding to that frequency is computed. The process is carried out numerically and iteratively.

In this study, making use of (i) the infinite series solution for the element transfer matrix given in equation (16), (ii) the Cayley–Hamilton principle, and (iii) the property of the differential matrix given in equation (14), an efficient numerical algorithm developed by Yıldırım [20, 21] is employed to yield the overall transfer matrix comprising the cases of great helix angles, large number of coils and different cross-sectional shapes. The present overall transfer matrix also includes the terms of both the axial and the shear deformations, and of the rotary inertia. The procedure for the algorithm considered is outlined below.

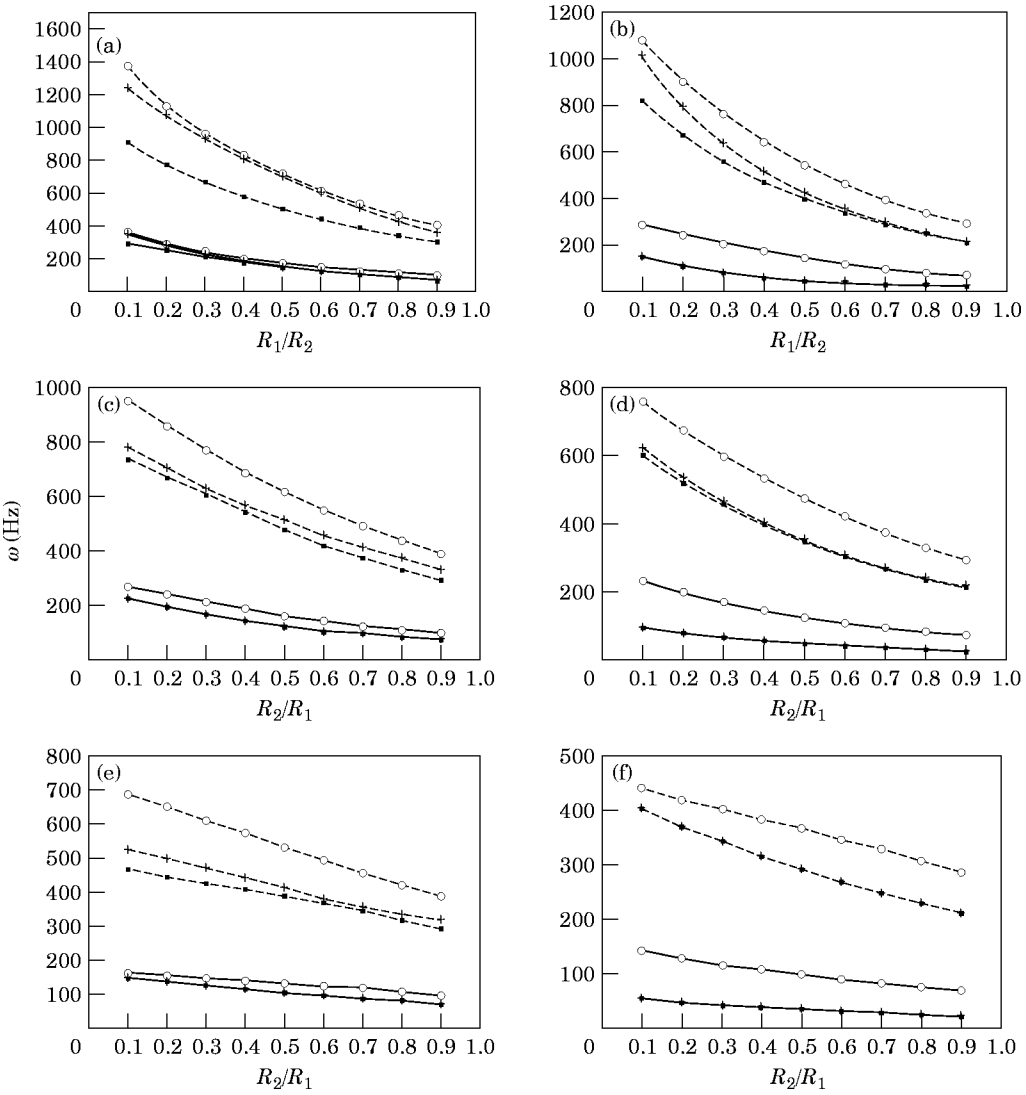

Figure 5. The effects of the helix pitch angle, the ratio R_{min}/R_{max} and the number of active turns on the natural frequencies, for $D_{max}/d = 10$. ---, $n_c = 5$; ———, $n_c = 15$. ■, ω_1; +, ω_2; ○, ω_3. (a) Hyperboloidal, $\alpha = 5°$, $D_2/d = 10$; (b) hyperboloidal, $\alpha = 15°$, $D_2/d = 10$; (c) conical, $\alpha = 5°$, $D_1/d = 10$; (d) conical, $\alpha = 15°$, $D_1/d = 10$, (e) barrel, $\alpha = 5°$, $D_1/d = 10$; (*f*) barrel, $\alpha = 15°$, $D_1/d = 10$.

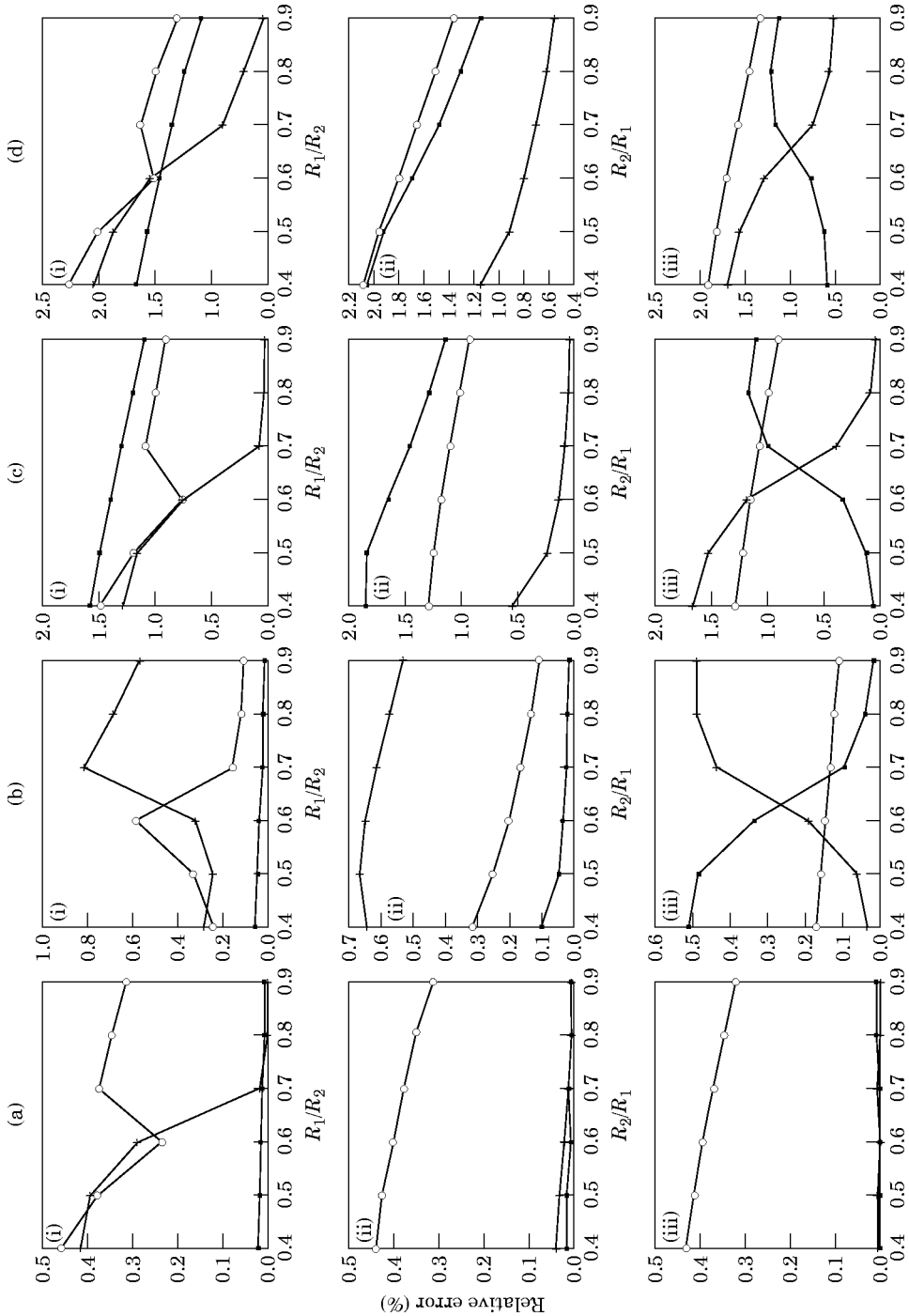

Figure 6. The effects of the rotary inertia and the axial and shear deformations on the free vibration frequencies, for $D_{max}/d = 5$, $\alpha = 5^\circ$ and $n_c = 5$. ■, ω_1; +, ω_2; ○, ω_3. (a) Excluding the axial deformation; (b) excluding the rotary inertia; (c) excluding the shear deformation; (d) excluding the rotary inertia and the axial and shear deformations. (i) Hyperboloidal; (ii) conical; (iii) barrel.

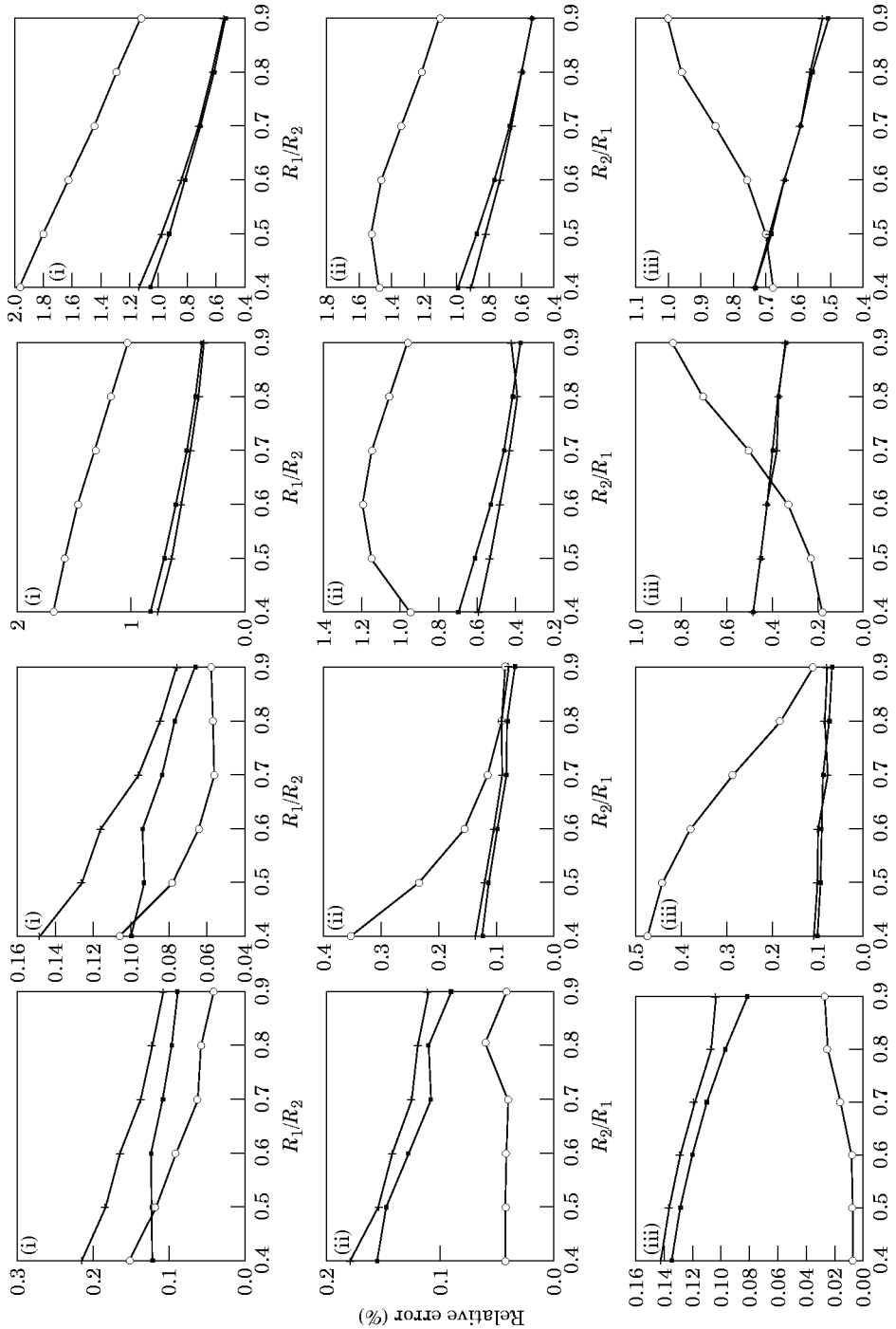

Figure 7. The effects of the rotary inertia and the axial and shear deformations on the free vibration frequencies, for $D_{max}/d = 5$, $\alpha = 15^\circ$ and $n_c = 5$. Key as for Figure 6.

To take into account the large pitch angles and rigid systems, the series solution of the transfer matrix can be arranged in a form that contains the finite powers of the differential matrix, using the Cayley–Hamilton theorem:

$$[F] = \Phi_1(\theta)[I] + \sum_{i=1}^{11} \Phi_{i+1}(\theta)[A^0]^i. \tag{19}$$

In equation (19), each function Φ of θ consists of infinite series. Denoting the last term which will be calculated in series by m, these functions can be expressed in terms of each element of series, $T_i^{(m)}$, as

$$\Phi_1(\theta) = 1 + T_1^{(0)} + T_1^{(1)} + T_1^{(2)} + \cdots + T_1^{(m)},$$

$$\Phi_i(\theta) = \frac{\theta^{i-1}}{(i-1)!} + T_i^{(0)} + T_i^{(1)} + T_i^{(2)} + \cdots + T_i^{(m)}, \qquad i = 2, 12, \tag{20}$$

where the terms, $T_i^{(m)}$, with zero-numbered superscripts, can be determined easily as follows:

$$T_{(2k+1)}^{(0)} = \frac{\theta^{12}}{12!} p_{(6-k)}, \qquad k = 0, 1, 2, \ldots, 5; \qquad T_{(2k)}^{(0)} = \frac{\theta^{13}}{13!} p_{(7-k)}, \qquad k = 1, 2, 3, \ldots, 6. \tag{21}$$

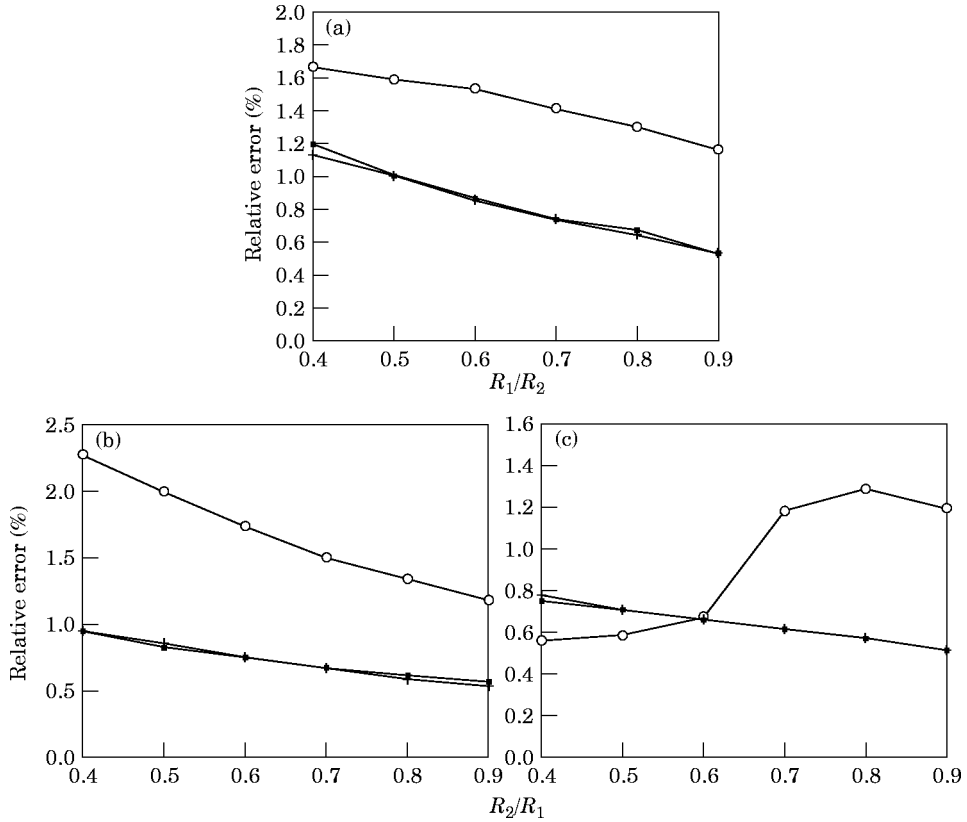

Figure 8. The effects of all the rotary inertia and the axial and shear deformations on the free vibration frequencies, for $D_{max}/d = 5$, $\alpha = 5^\circ$ and $n_c = 15$. ■, ω_1; +, ω_2; ○, ω_3. (a) Hyperboloidal; (b) conical; (c) barrel.

It is evident that the numerical transfer matrix cannot be calculated accurately unless numerous terms are added to the series. For this reason, some preventive measures against the overflow limit of computer must be taken during the computation. In this study, as a result of lengthy manipulations, the relationship between any two consecutive terms has been obtained and given below:

$$T^{(n)}_{(2k+1)} = \frac{\theta^2}{(11+2n)(12+2n)} \{T^{(n-1)}_{(11)} p_{(6-k)} + T^{(n-1)}_{(2k-1)}\}, \qquad k = 0, 1, 2, \ldots, 5;$$

$$T^{(n)}_{(2k)} = \frac{\theta^2}{(12+2n)(13+2n)} \{T^{(n-1)}_{(12)} p_{(7-k)} + T^{(n-1)}_{(2k-2)}\}, \qquad k = 1, 2, 3, \ldots, 6. \tag{22}$$

4. TEST PROBLEMS

For the purpose of computing the natural frequencies of cylindrical or non-cylindrical helical springs, a computer program coded in Fortran has been devised. With the help of this program, miscellaneous problems have been solved and their results are given below.

4.1. CYLINDRICAL HELIX

First, in order to illustrate the efficiency of the numerical algorithm which is capable of calculating the overall transfer matrix in an accurate manner, a cylindrical helical

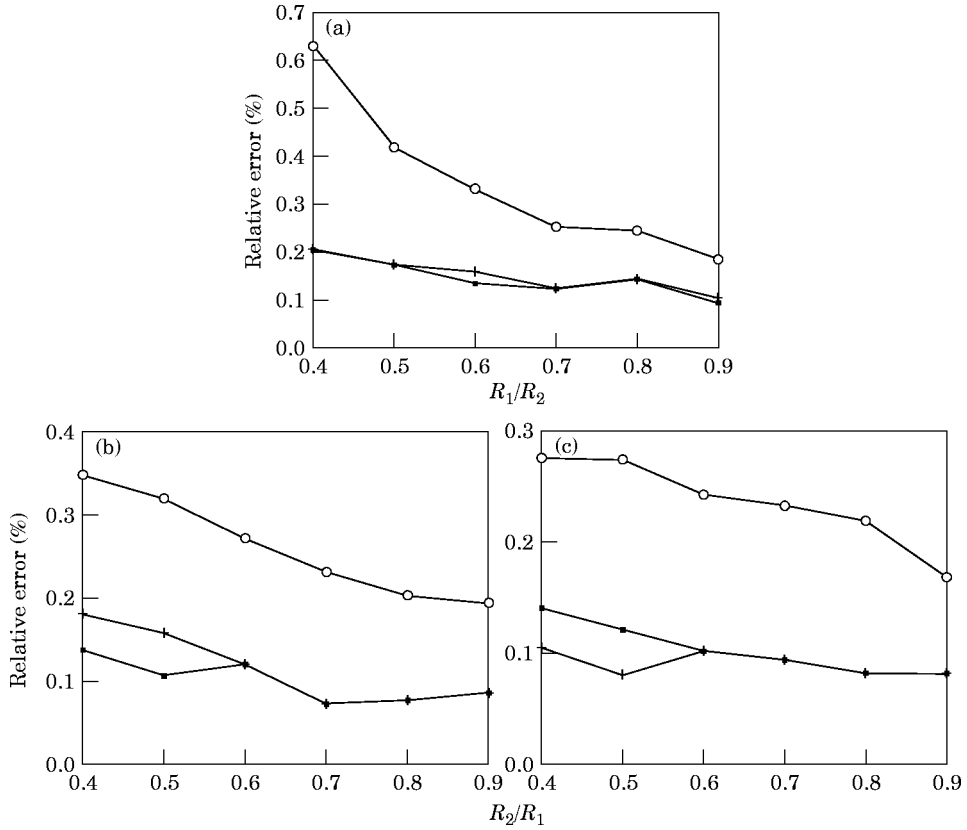

Figure 9. The effects of all the rotary inertia and the axial and shear deformations on the free vibration frequencies, for $D_{max}/d = 5$, $\alpha = 15^\circ$ and $n_c = 15$. Key as for Figure 8.

spring fixed at both ends has been considered. The results are presented in Table 1. Satisfactory agreement is evident from Table 1.

4.2. NON-CYLINDRICAL HELICES

In order to show the convergence of the theoretical results obtained to the exact solution, a hyperboloidal type spring fixed at both ends has been chosen. The material and geometrical properties of the spring are: $d = 2{\cdot}6$ mm, $R_1 = 13$ mm, $n_c = 6{\cdot}5$, $\alpha = 4{\cdot}8^\circ$, $\rho = 7850$ kg/m^3, $E = 2{\cdot}1 \times 10^{11}$ N/m^2, $v = 0{\cdot}3$, $\alpha_n = \alpha_b = 1{\cdot}1$.

Variation of the frequencies of the spring with respect to the number of elements is presented in Table 2. It is clearly seen from Table 2 that the results obtained by the present program converge more rapidly. Acceptable results can be computed even if one circle of the coil is divided into two segments. However, in order to reduce geometric errors, which will occur especially during the computation of the higher frequencies for small ratios of R_2/R_1, 50 elements was found to be adequate.

Other numerical solutions obtained for 50 elements of hyperboloidal spring having different ratios of R_2/R_1 are given in Table 3. The same problem has also been treated by Nagaya *et al*. [23] both experimentally and theoretically using the Myklestad method. Since the results had not been presented numerically in that paper, the numerical values of the frequencies have been obtained approximately from their graphs for comparison. Inspection of Table 3 clearly indicates that their experimental and numerical results are in close proximity to the present results.

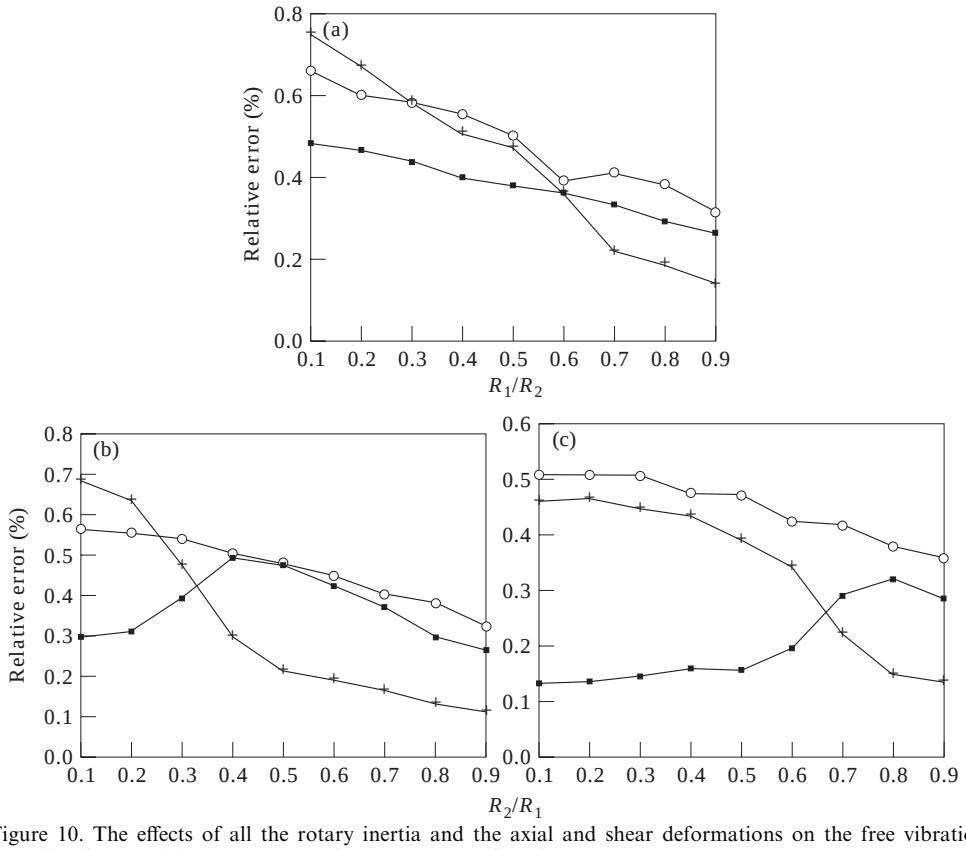

Figure 10. The effects of all the rotary inertia and the axial and shear deformations on the free vibration frequencies, for $D_{max}/d = 10$, $\alpha = 5^\circ$ and $n_c = 5$. Key as for Figure 8.

For the second non-cylindrical example, a barrel type spring is considered. The properties of the spring are as follows: $R_1 = 25$ mm, $\alpha = 4{\cdot}8^\circ$, $n = 6{\cdot}5$, $E = 2{\cdot}1 \times 10^{11}$ N/m^2, $\rho = 7850$ kg/m^3, $v = 0{\cdot}3$, $d = 2$ mm, $\alpha_n = \alpha_b = 1{\cdot}1$. This problem has also been studied by Nagaya *et al*. [23] using the Myklestad method. They have taken into account only the axial deformation, and neglected the rotary inertia. They have solved this problem by dividing every coil into 12 segments. Their results, obtained theoretically and experimentally, have also been presented in graphical form. A close agreement between the results computed in the present study which are given in Table 4 and some of their results is evident. It is observed from their graphics that they have missed frequencies associated with the third and fourth modes. Although these frequencies might have been computed, they have not been presented. As can be observed from Table 4, the third and fourth frequencies of the barrel spring are very close to each other. In general, determination of these frequencies experimentally is very difficult. There is a very good agreement between the results of the present study and Yıldırım [25].

The material and geometrical properties of the conical spring considered as a third non-cylindrical example are the same as in the previous example. The numerical results pertaining to this problem are given in Table 5.

As a fourth non-cylindrical example the hyperboloidal type spring is considered again in order to compare the frequencies of springs having different irregular shapes and the same largest radius of circle, $R_{max} = D_{max}/2$. The features of this spring are the same as those for the third example. The frequencies of this example are shown in Table 6.

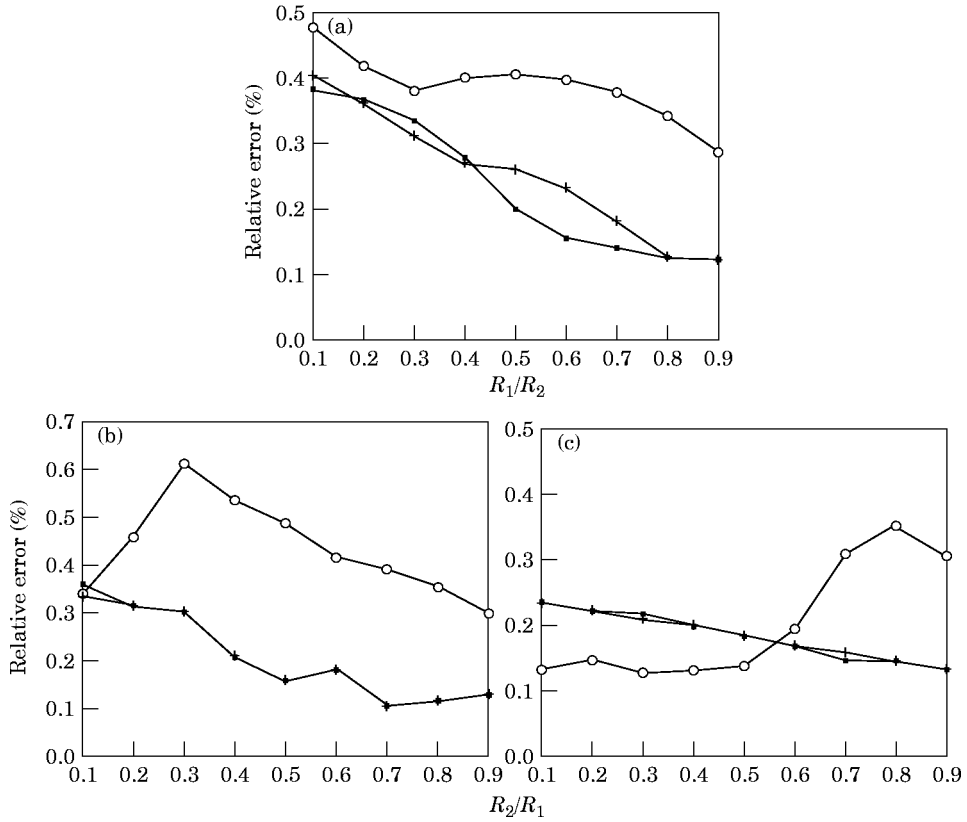

Figure 11. The effects of all the rotary inertia and the axial and shear deformations on the free vibration frequencies, for $D_{max}/d = 10$, $\alpha = 5^\circ$ and $n_c = 15$. Key as for Figure 8.

While some frequencies are very close to each other for the barrel spring (Table 4), considerable divergences has been found in the case of other types (Tables 5 and 6).

In Figure 3 is shown the variation with R_1/R_2 (or R_2/R_1) of two frequencies of various types of helices. As seen from the figure, the hyperboloidal spring is more rigid than other types of helices for the same constant largest radius and properties of material. As the mode number increases, the difference between the frequencies which depends on the type of helices is increased. The frequencies of springs can be sorted in ascending order as cylindrical, barrel, conical and hyperboloidal.

5. EFFECTS OF THE NUMBER OF ACTIVE TURNS, THE HELIX PITCH ANGLE, AND THE RATIO OF (D_{max}/d) ON THE NATURAL FREQUENCIES

In this section, the effects of the vibrational parameters chosen such as the helix pitch angle, the ratio of (D_{max}/d), and the number of active turns on the free vibration frequencies of non-cylindrical helical springs are studied. The results are given in Figures 4 and 5 for the properties of the spring of circular section: $\rho = 7850\ \text{kg/m}^3$, $E = 2{\cdot}1 \times 10^{11}\ \text{N/m}^2$, $v = 0{\cdot}3$, $\alpha_n = \alpha_b = 1.1$, $d = 2{\cdot}6$ mm. There is no physical meaning of the ratio of (R_{min}/R_{max}) less than 0·4 for the ratio of $(D_{max}/d = 5)$. As can be observed in these figures, as the helix angle increases the natural frequencies of all types of helices decrease when all the other spring properties are kept constant. If the helix angle increases, the total length of the spring increases, consequently, the stiffness of the spring decreases. When the helix angle increases, coupled modes begin to emerge. Similarly, as the number of active turns increases, the spring length increases, and the natural frequencies decrease. Coupled modes begin to appear with increasing n_c. Similar characteristic frequency curves are obtained for both the ratios $(D_{max}/d = 5)$ and $(D_{max}/d = 10)$.

6. THE EFFECTS OF THE ROTARY INERTIA, AXIAL AND SHEAR DEFORMATIONS ON THE NATURAL FREQUENCIES

In this section relative errors are finally computed to determine the effects of the rotary inertia, the axial and shear deformation terms on the natural frequencies of all types of helices. In Figures 6(a)–(c) is shown the effect of neglecting the axial deformation, the rotary inertia and the shear deformation, respectively, for $D_{max}/d = 5$, $n_c = 5$ and $\alpha = 5^\circ$. In Figure 6(d) is shown the relative error when all of the above are neglected. Figure 7 demonstrates the similar cases for $D_{max}/d = 5$, $n_c = 5$ and $\alpha = 15^\circ$. It is observed from the figures that the effect of the shear deformation is predominant over the others. The effect of each term is to be significant for any one of the natural frequencies which varies with respect to the value of both α and the ratio R_{min}/R_{max}. In this respect, taking the final decision may be inadequate. The effect of the rotary inertia terms is generally of more importance than the effect of the axial deformation. The maximum total relative error is observed as approximately 2·5% for hyperboloidal type spring.

The effects of the rotary inertia, axial and shear deformation terms are demonstrated in Figures 8–11. As can be expected, these effects decrease with increasing α, D_{max}/d and n_c.

In this section only the first three frequencies are considered. These effects can be more considerable at higher frequencies.

7. CONCLUSIONS

In the present work, the free vibration frequencies of non-cylindrical helices comprising the effects of both axial and shear deformations and the rotary inertia have been

determined theoretically by the transfer matrix method. To the knowledge of the authors, the results obtained using the numerical algorithm given in section 3 are the closest to the experimental data available in the open literature. The algorithm presented can be used efficiently for the determination of the free vibration frequencies of the springs of irregular shapes. In this study, 300 terms have been taken while determining each Φ function, equations (19) and (20), for calculation of the element transfer matrix. This corresponds to $300 \times 12 = 3600$ terms in equation (16). If equation (16) had been used, the factorial of 3600 should have been computed. However, this can be avoided with the help of some numerical manipulations, such as those used in this study. Although 300 terms was thought to be enough for the examples considered here, it is possible to increase this number if required.

REFERENCES

1. A. M. Wahl 1963 *Mechanical Springs*. New York: McGraw-Hill.
2. W. H. Wittrick 1966 *International Journal of Mechanical Sciences* **8**, 25–47. On elastic wave propagation in helical springs.
3. Y. Kagawa 1968 *Journal of Sound and Vibration* **8**, 1–15. On the dynamical properties of helical springs of finite length with small pitch.
4. K. K. Pujara and Y. Kagawa 1971 *Slovakian Journal* **1**, 68–79. Phase velocities and displacement characteristics of free waves along a helical spring.
5. J. W. Philips and G. A. Costello 1972 *Journal of the Acoustical Society of America* **51**, 967–973. Large deflection of impacted helical springs.
6. G. A. Costello 1975 *Transactions of the American Society of Mechanical Engineers*, *Journal of Applied Mechanics* **42**, 789–792. Radial expansion of impacted helical springs.
7. L. Della Pietra 1976 *Meccanica* **11**, 102–119. The dynamic coupling of torsional and flexural strains in cylindrical helical springs.
8. A. R. Guido, L. Della Pietra and S. Della Valle 1978 *Meccanica* **13**, 90–108. Transverse vibrations of cylindrical helical springs.
9. J. E. Mottershead 1980 *International Journal of Mechanical Sciences* **22**, 267–283. Finite elements for dynamical analysis of helical rods.
10. J. E. Mottershead 1982 *International Journal of Mechanical Sciences* **24**, 547–558. The large displacements and dynamic stability of springs using helical finite elements.
11. L. Della Pietra and S. Della Valle 1982 *Meccanica* **17**, 31–43. On the dynamic behaviour of axially excited helical springs.
12. D. Pearson 1982 *International Journal of Mechanical Sciences* **24**, 163–171. The transfer matrix method for the vibration of compressed helical springs.
13. T. Sawanobori and Y. Fukushima 1983 *Transactions of the Japan Society of Mechanical Engineers* **49**, 422–428. Analysis of dynamic behaviours of coil springs (in Japanese).
14. T. Sawanobori and Y. Fukushima 1983 *Bulletin of the Japan Society of Mechanical Engineers* **26**, 2002–2009. A finite element approach to dynamic characteristics of helical springs (free vibration).
15. D. Pearson and W. H. Wittrick 1986 *International Journal of Mechanical Sciences* **28**, 83–96. An exact solution for the vibration of helical springs using a Bernoulli-Euler model.
16. Y. Lin and A. P. Pisano 1987 *Journal of Applied Mechanics* **54**, 910–917. General dynamic equations of helical springs with static solution and experimental verification.
17. H. S. Tsay and H. B. Kingsbury 1988 *Journal of Sound and Vibration* **124**, 539–554. Vibrations of rods with general space curvature.
18. W. Jiang, W. K. Jones, T. L. Wang and K. H. Wu 1991 *International Journal of Mechanical Sciences* **58**, 222–228. Free vibrations of helical springs.
19. Y. Xiong and B. Taborrok 1992 *International Journal of Mechanical Sciences* **34**, 41–51. A finite element method for the vibration of spatial rods under various applied loads.
20. V. Yildirim 1995 *Turkish Journal of Engineering and Environmental Sciences* **19**, 343–356. Investigation of free vibration of helical springs by the stiffness matrix method (in Turkish).
21. V. Yildirim 1996 *International Journal of Numerical Methods in Engineering* **39**, 99–114. Investigation of parameters affecting free vibration frequency of helical springs.
22. I. Epstein 1947 *Journal of Applied Physics* **18**, 368–374. The motion of a conical coil spring.

23. K. NAGAYA, S. TAKEDA and Y. NAKATA 1986 *International Journal for Numerical Methods in Engineering* **23**, 1081–1099. Free vibration of coil spring of arbitrary shape.
24. V. YILDIRIM 1996 *Turkish Journal of Engineering and Environmental Sciences* **20**, 121–128. The Myklestad method for the free vibration of non-cylindrical helical springs (in Turkish).
25. V. YILDIRIM 1997 *Communications in Numerical Methods in Engineering* (to be published). Free vibration analysis of non-cyklindrical coil springs by combined use of the transfer matrix and the complementary functions methods.
26. F. R. GANTMACHER 1960 *The Theory of Matrices*. New York: Chelsea.